DIRECT SIMULATION FOR WIND INSTRUMENT SYNTHESIS

Stefan Bilbao[*]
Music/Acoustics and Fluid Dynamics Group,
University of Edinburgh
Edinburgh, UK
sbilbao@staffmail.ed.ac.uk

ABSTRACT

There are now a number of methods available for generating synthetic sound based on physical models of wind instruments, including digital waveguides, wave digital filters, impedance-based methods and those involving impulse responses. Normally such methods are used to simulate the behaviour of the resonator, and the coupling to the excitation mechanism is carried out by making use of simple lumped finite difference schemes or digital filter structures. In almost all cases, a traveling wave, frequency-domain, or impulse response description of the resonator is used as a starting point—efficient structures may be arrived at when the bore is of a particularly simple form, such as a cylinder or cone.

In recent years, however, due to the great computing power available, efficiency has become less of a concern—this is especially the case for musical instruments which may be well-modelled in 1D, such as wind instruments. In this paper, a fully time-space discrete algorithm for the simulation and synthesis of woodwind instrument sounds is presented; such a method, though somewhat more computationally intensive than an efficient waveguide structure, is still well within the realm of real-time performance. The main benefits of such a method are its generality (it is no longer necessary to make any assumptions about bore profile, which may be handled in an almost trivial manner), extensibility (i.e., the model may be generalized to handle nonlinear phenomena directly), ease of programming, and the possibility of direct proofs of numerical stability without invoking frequency domain concepts.

Simulation results, sound examples and a graphical user interface, in the Matlab programming language are also presented.

1. INTRODUCTION

The synthesis of sound based on physical models of wind instruments has traditionally been carried out in a variety of ways. Digital waveguides [1, 2] have been extensively explored, especially in the special cases of cylindrical and conical tubes, in which case they yield an extreme efficiency advantage. A related scattering method, wave digital filtering [3], is also used in order to connect waveguide tube models with lumped elements such as an excitation mechanism [4] or toneholes [5]. Another body of techniques, closely related to digital waveguides, and based around impedance descriptions, has been developed by Guillemain and his associates [6]. Other techniques, based on the so-called "K"-method (in opposition to wave- and scattering-based methods) bear a closer resemblance to the direct simulation methods to be discusssed here [7]. Most of these methods owe a great deal to the much earlier treatment of self-sustained musical oscillators due to McIntyre, Schumacher and Woodhouse [8].

All of these methods rely, to some degree, on simplified descriptions of the resonator (tube)—for example, digital waveguides make use of a traveling wave decomposition, accompanied by frequency-domain (impedance or reflectance) characterizations of lumped elements or phenomena such as bell radiation and tone holes. Other methods make use of impedance descriptions of the resonator itself [6], or, its time-domain counterpart, the Green's function [8]. Such points of view follow directly from investigations in pure musical acoustics, and are of course indispensible as analysis tools. When it comes to sound synthesis, however, it is not clear that they are necessary—once one has arrived at a satisfactory model of a musical instrument, written as a time-space PDE system (for the resonator) coupled to ODEs (the excitation element and a radiation boundary condition), one may proceed directly to a synthesis algorithm without invoking any notion of frequency, impedance, wave variables, or reflectance. Though one of course loses the powerful analysis perspective mentioned above, the treatment of the resonator becomes independent of any particular bore profile, and the system as a whole is now much more amenable to interesting extensions involving, e.g., time-varying and nonlinear effects which do indeed play a role in wind instruments, and which are not easily approached using impedance or scattering concepts. In the present case, concerned with audio synthesis (and thus efficiency), the model remains 1D; for more on the use of standard numerical techniques in multi-D, in the setting of acoustical analysis of musical instruments, see. e.g., [9].

A standard model of a reed wind instrument is presented in Section 2, followed by a development of a finite difference time domain algorithm in Section 3, including some discussion of implemntation details, such as the operation count, and computability issues. In Section 4, simulation results are presented, and in Section 5, a graphical user interface, in the Matlab environment, is exhibited.

2. A STANDARD WIND INSTRUMENT MODEL

2.1. Instrument Body

A standard model of one-dimensional linear wave propagation in an acoustic tube [10] is given by the following set of equations:

$$\frac{\rho}{S}u_t = -p_x \qquad \frac{S}{\rho c^2}p_t = -u_x \qquad t \geq 0, x \in [0, L] \qquad (1)$$

Here, $u(x,t)$ and $p(x,t)$ are the volume velocity and pressure, respectively, at position x, and at time t, and subscripts t and x refer

[*] This work was supported by the Engineering and Physical Sciences Council UK, under grant number C007328/1, the Leverhulme Trust, and the CONSONNES project.

to time and space differentiation, respectively. ρ and c are the density and wave speed, respectively, $S(x)$ is the tube cross-sectional area at position x, and L is the length of the tube. See Figure 1. The system above is sometimes condensed into a single second order system, known as Webster's equation [11]; it is also the starting point for various speech synthesis algorithms [12], including the Kelly-Lochbaum model [13].

This model results from many simplifying assumptions, the most important of which are linearity, relatively slow variation in $S(x)$ and the size of $S(x)$ relative to audio wavelengths, and losslessness. For more comments on these assumptions (some more justifiable than others), see Section 6.

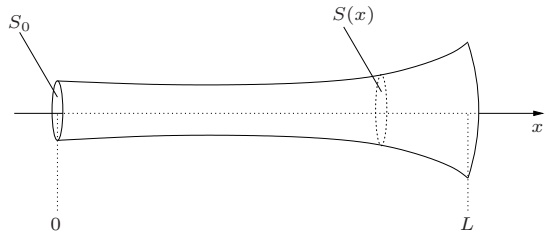

Figure 1: *Acoustic tube of variable cross-sectional area* $S(x)$

It is useful to dimensionally reduce the problem, by introducing the variables $x' = x/L$, $p' = p/\rho c^2$, and $u' = u/cS_0$, as well as a dimensionless area function $S' = S/S_0$, where S_0 is a reference surface area, such as $S_0 = S(x = 0)$. This leads, after substitution in (1) and removal of primes, to

$$\frac{1}{S}u_t = -\gamma p_x \qquad Sp_t = -\gamma u_x \qquad t \geq 0, x \in [0, 1] \tag{2}$$

where $\gamma = c/L$. The lowest resonant frequency of the tube will be on the order of γ. Initial conditions for the system may be set to zero, and proper boundary conditions (one required at each end of the domain) follow from the consideration of the reed excitation and bell radiation, to be discussed shortly.

2.2. Reed Mechanism

A slightly non-standard model of reed vibration may be given as follows (see Figure 2). For a one-mass model, the reed displacement behaves according to

$$\ddot{y} + g\dot{y} + \omega_0^2(y - y_0) - \frac{\omega_1^\alpha}{y_0^{\alpha-2}}\left(|y^-|\right)^{\alpha-1} = -\frac{S_r \Delta p}{M_r} \tag{3}$$

Here, $y(t)$ is the displacement of the reed relative to an equilibrium position y_0, M_r is the reed mass, S_r an effective surface area of the reed, ω_0 the resonant frequency, and g a damping parameter. Dots above variables signify total time differentiation. The term involving the coefficient ω_1 models the collision of the reed with the mouthpiece. It becomes active when $y < 0$, and acts as a one-sided repelling force, modelled as a power-law nonlinearity, of exponent α. Here, $y^- = (y - |y|)/2$. The reed displacement y is thus here permitted to be negative. This term, inspired by collision models used in hammer-string dynamics [14], is the sole distinguishing feature of the model, which is otherwise identical to that which appears in the literature [15, 16, 17].

The oscillator above is driven by the pressure difference Δp, given by

$$\Delta p = p_m - p_{in}$$

where $p_m(t)$ is the mouth pressure, and $p_{in}(t)$ the pressure at the entrance to the acoustic tube. The pressure difference is related to the flow in the mouthpiece u_m through Bernoulli's law,

$$u_m = wy^+\sqrt{\frac{2|\Delta p|}{\rho}}\text{sign}(\Delta p) \tag{4}$$

where here, w is the width of the reed channel. The flow is nonzero only when the reed is not in contact with the mouthpiece, or when $y > 0$. As such, the quantity y^+ is given by $y^+ = (y + |y|)/2$. Neglected here is an inertia term—see, e.g., [11]. The square root dependence of flow on velocity could be generalized to a power law [18] with few resulting complications in the discretization procedure to be outlined below.

The flow variables themselves are related by a conservation law

$$u_{in} = u_m - u_r$$

where u_{in} is the flow entering the acoustic tube, and where u_r is related to reed displacement y by

$$u_r = S_r\dot{y}$$

It is useful to introduce scaled variables as follows:

$$y' = \frac{y}{y_0} - 1 \qquad p'_\cdot = \frac{p_\cdot}{\rho c^2} \qquad u'_\cdot = \frac{u_\cdot}{cS_0}$$

for any pressure variable $p_\cdot$ or velocity variable $u_\cdot$, which, when inserted in the above equations (and primes subsequently removed) lead to the system:

$$\ddot{y} + g\dot{y} + \omega_0^2 y - \omega_1^\alpha\left(|(y+1)^-|\right)^{\alpha-1} = -\mathcal{Q}\Delta p \tag{5a}$$

$$\Delta p = p_m - p_{in} \tag{5b}$$

$$u_m = \mathcal{R}(y+1)^+\sqrt{|\Delta p|}\text{sign}(\Delta p) \tag{5c}$$

$$u_{in} = u_m - u_r \tag{5d}$$

$$u_r = \mathcal{S}\dot{y} \tag{5e}$$

where

$$\mathcal{Q} = \frac{\rho c^2 S_r}{M_r y_0} \qquad \mathcal{R} = \sqrt{2}\frac{wy_0}{S_0} \qquad \mathcal{S} = \frac{S_r y_0}{cS_0}$$

Note that higher-order effects of the time variation of y_0 (which is possible during play), which is generally quite slow, are neglected here, as in previous treatments of the reed system [15].

It should be clear that in a connection with the acoustic tube described by (2), it must be true that

$$p(0,t) = p_{in}(t) \qquad u(0,t) = u_{in}(t) \tag{6}$$

2.3. Bell Radiation

One boundary condition is required at the bell termination. Normally, in the musical acoustics literature (see, e.g., [11, 19]), one employs the standard radiation impedance result for an unflanged tube. Often, this is given, in the low-frequency limit, in a polynomial form obtained through a series approximation. While this is fine for analysis purposes, positive realness [20] (and thus passivity) is lost, and numerical instabilities can arise in simulation. It is thus better, in this context, to make use of a rational and positive real approximation to the radiation impedance (see, e.g., the

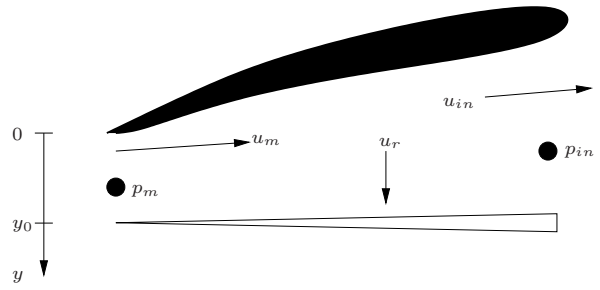

Figure 2: *Pressure and flow variables in a reed instrument mouthpiece.*

form given in [12]), leading to the following relationship between scaled pressure and velocity at $x = 1$:

$$u(1,t) = m + \beta p(1,t) \qquad \dot{m} = \alpha p(1,t) \tag{7}$$

where $m(t)$ is an auxiliary variable, and where the constants α and β are given by

$$\alpha = \frac{3\gamma L}{8}\sqrt{\frac{\pi^3 S(1)}{S_0}} \qquad \beta = \frac{9\pi^2 S(1)}{128}$$

The term with coefficient α corresponds to the reactive part of the radiation impedance, and that with coefficient β to the resistive part. The extra variable m is necessary, in the discrete setting, in order to accommodate the extra energy storage required by a reactive termination. One could go much further here, and develop boundary conditions which model radiation to higher accuracy (thus requiring more state), but the positive realness criterion must continue to be enforced (i.e., a higher order polynomial series approximation to the radiation impedance will not suffice). Positive realness of an impedance corresponds directly to bounded realness for the associate reflectance, a quantity which is probably better known to musical acousticians.

3. A SIMPLE FINITE DIFFERENCE SCHEME

A finite difference time domain scheme for system (1) is similar to that which appears in 1D electromagnetics simulation [21, 22], with the slight added complication of spatial variation in the parameters (i.e., the surface area $S(x)$). Introduce staggered grid functions $p_l^{n+1/2}$, and $u_{l+1/2}^n$, for integer l and n; these are approximations to $p(x,t)$ and $u(x,t)$ at locations $(x = lh, t = (n+\frac{1}{2})k)$ and $(x = (l+\frac{1}{2})h, t = nk)$, respectively, where h and k are the spacing between adjacent grid points and time step, respectively. See Figure 3. k is related to the sample rate f_s by $k = 1/f_s$—in audio synthesis applications, k is thus normally chosen a priori. The resulting scheme is of the following form:

$$\left[\frac{1}{S}\right]_{l+\frac{1}{2}} \left(u_{l+\frac{1}{2}}^{n+1} - u_{l+\frac{1}{2}}^{n}\right) = -\lambda\left(p_{l+1}^{n+\frac{1}{2}} - p_l^{n+\frac{1}{2}}\right) \tag{8a}$$

$$[S]_l \left(p_l^{n+\frac{1}{2}} - p_l^{n-\frac{1}{2}}\right) = -\lambda\left(u_{l+\frac{1}{2}}^{n} - u_{l-\frac{1}{2}}^{n}\right) \tag{8b}$$

where the Courant number λ is defined as $\lambda = k\gamma/h$, and where $\left[\frac{1}{S}\right]_{l+\frac{1}{2}}$ and $[S]_l$ are approximations to the continuous function $S(x)$ at locations $x = (l+\frac{1}{2})h$ and $x = lh$, respectively. Under the special choices

$$\left[\frac{1}{S}\right]_{l+\frac{1}{2}} = \frac{2}{S(lh) + S((l+1)h)} \tag{9}$$

$$[S]_l = \frac{1}{4}\left(S((l-1)h) + 2S(lh) + S((l+1)h)\right) \tag{10}$$

a necessary condition for numerical stability becomes

$$\lambda \leq 1 \tag{11}$$

This is the familiar Courant-Friedrichs-Lewy condition [23, 24], arrived at through energy techniques (and not frequency or von Neumann analysis, which is not generally applicable to problems with spatial variation [25])—note that the condition is independent of the variation in S itself, simplifying implementation somewhat.

In particular, for a given time step k, the grid spacing h must be chosen so as to divide the unit interval into an integer number of parts, and it is also important that (11) be satisfied as near to equality as possibility. This leads to the choice

$$N = \text{floor}\,(1/\gamma k) \qquad h = 1/N$$

The scheme (8) is a one-step scheme in the two grid functions p and u, and is formally second-order accurate. As illustrated in Figure 3, the grid function $p_l^{n+\frac{1}{2}}$ is defined for $l = 0, \ldots, N$, and $u_{l+\frac{1}{2}}^n$ for $l = -1, \ldots, N$. Thus updating of p, according to (8b) may be performed directly, but updating of u, according to (8a), at grid locations $-h/2$ and $N + h/2$ necessarily requires a boundary condition—this will be discussed shortly.

3.1. Scheme for Reed System

For the reed system, given in (5), consider the following scheme:

$$\frac{1}{k^2}\left(y^{n+1} - 2y^n + y^{n-1}\right) + \frac{g}{2k}\left(y^{n+1} - y^{n-1}\right) + \frac{\omega_0^2}{2}\left(y^{n+1} + y^{n-1}\right) + \frac{\omega_1^\alpha}{2}|(y^n+1)^-|^{\alpha-2}\left(y^{n+1} + y^{n-1}\right) = -\mathcal{Q}\Delta p^n \tag{12a}$$

$$\Delta p^n = p_m^n - p_{in}^n \tag{12b}$$

$$u_m^n = \mathcal{R}(y^n+1)^+\sqrt{|\Delta p^n|}\text{sign}(\Delta p^n) \tag{12c}$$

$$u_{in}^n = u_m^n - u_r^n \tag{12d}$$

$$u_r^n = \frac{\mathcal{S}}{2k}\left(y^{n+1} - y^{n-1}\right) \tag{12e}$$

Here, the functions y, u_m, u_r, u_{in}, p_m, p_{in}, and Δp have been approximated by time series, with time step k. p_m, in particular, is assumed to be a known input control signal, and p_{in} and u_{in} will be related to values of the grid function in p and u over the problem interior. Worth noting here is the approximation to the stiffness term (with coefficient ω_0^2) and the collision term (with coefficient ω_1^α), both of which make use of semi-implicit discretizations. Such implicit approximations, when applied to lumped systems such as the reed, significantly ease stability requirements, and, as long as the unknown value of the grid function appears linearly (as it does here) still allows for fully explicit updating—see Section 3.3. To this end, it is worth reducing the system above to

$$\Delta p^n + a_1^n\sqrt{|\Delta p^n|}\text{sign}\,(\Delta p^n) + a_2^n = a_3^n u_{in}^n \tag{13}$$

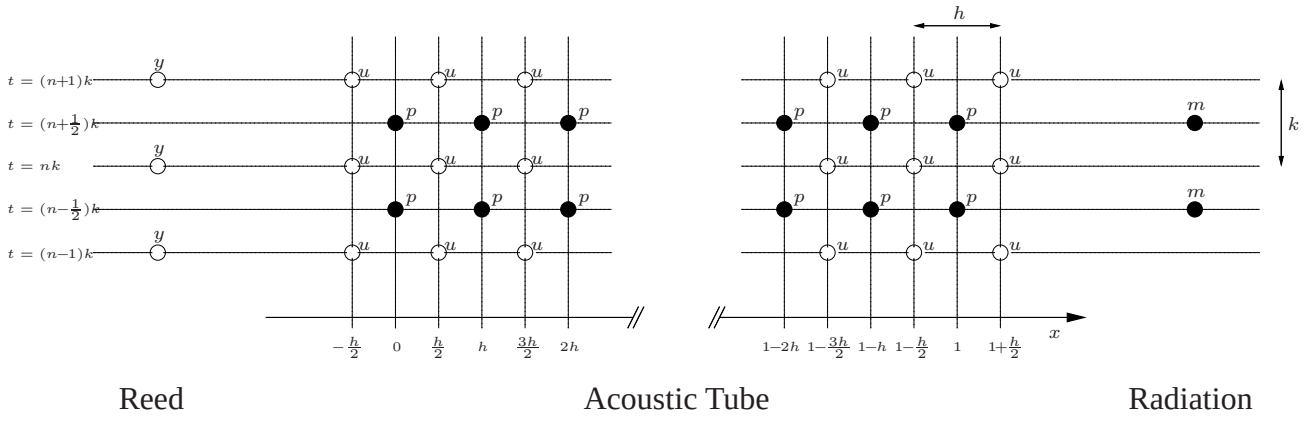

Figure 3: *Staggered grid for finite difference scheme* (8) *for acoustic tube.*

where the coefficients $a_1^n \geq 0$, a_2^n and $a_3^n \geq 0$ will depend on known (previously computed) values of y^n and the various defining parameters of the reed system. (The non-negativity of a_1^n and a_3^n, follows from the use of semi-implicit discretizations to the stiffness terms.)

In order to couple the reed system to the acoustic tube, one possible approximation to (6) is

$$u_{in}^n = u_{-\frac{1}{2}}^n \qquad p_{in}^n = \frac{1}{2}\left(p_0^{n+\frac{1}{2}} + p_0^{n-\frac{1}{2}}\right) \tag{14}$$

From the update (8b) at grid point $l = 0$, and using the above conditions, as well as (12b), one may arrive at the relation

$$\Delta p^n = b_1^n - b_2^n u_{in}^n \tag{15}$$

where again, b_1^n and $b_2^n \geq 0$ depend on previously computed values of the grid functions p and u, as well as the input pressure p_m. Now, (13) and (15) may be combined into a single equation for the pressure difference Δp^n:

$$|\Delta p^n| + c_1^n \sqrt{|\Delta p^n|} + \frac{c_2^n}{\text{sign}\,(\Delta p^n)} = 0 \tag{16}$$

for the coefficents $c_1^n \geq 0$ and c_2^n. One may then observe that, in order for a solution to exist, one must have $\text{sign}\,(\Delta p^n) = -\text{sign}\,(c_2^n)$, at which point the magnitude $|\Delta p^n|$ may be determined uniquely. In this case, due to the form of the pressure-flow characteristic (4), this may be done using the quadratic formula, a unique solution will exist for any such characteristic which is one-to-one, though an iterative method (necessarily convergent) may be necessary. In this sense, finite difference updating is simpler than in the closely related case of the bow-string interaction (in which case the force-velocity characteristic is not necessarily one-to-one) [25].

3.2. Scheme at Bell Termination

For the bell termination, an approximation to the boundary condition (7) is given by

$$\begin{aligned} u_{N+\frac{1}{2}}^n &= \frac{\beta}{2}\left(p_N^{n-\frac{1}{2}} + p_N^{n+\frac{1}{2}}\right) + \frac{1}{2}\left(m^{n+\frac{1}{2}} + m^{n-\frac{1}{2}}\right) \\ m^{n+\frac{1}{2}} &= m^{n-\frac{1}{2}} + \frac{k\alpha}{2}\left(p_N^{n-\frac{1}{2}} + p_N^{n+\frac{1}{2}}\right) \end{aligned} \tag{17}$$

Again, as in the case of the reed termination, the unknowns, $u_{N+\frac{1}{2}}^n$ and $p_N^{n+\frac{1}{2}}$ are coupled. In this case, though, the coupling is linear. Employing scheme (8b) at grid location $l = N$ leads to a unique solution for $u_{N+\frac{1}{2}}^n$ in terms of previously computed values of the grid functions p and u, as well as m, i.e.,

$$u_{N+\frac{1}{2}}^n = d^n \tag{18}$$

where d^n depends on previously computed values of the grid functions p and u, as well as m.

3.3. Explicit Updating

It is important to point out that, despite the apparently complex relationship among the stored variables at the terminations and the grid function to be updated over the interior, a purely explicit update form may be arrived at, but the order in which operations are performed is of great importance. Consider the entire scheme at the end of an update cycle, at which point all values at time step n or previously are known, except for the values $u_{-\frac{1}{2}}^n$ and $u_{N+\frac{1}{2}}^n$. One may then proceed as follows:

- Calculate Δp^n from (16).
- Calculate y^{n+1} using Δp^n, from (12a).
- Calculate u_r^n from (12e).
- Calculate u_m^n from (12c).
- Calculate u_{in}^n from (12d), and set $u_{-\frac{1}{2}}^n$ from (14).
- Calculate $u_{N+\frac{1}{2}}$ from (18).
- Calculate $p_l^{n+\frac{1}{2}}$, for $l = 0, \ldots, N$, from (8b).
- Calculate $m^{n+\frac{1}{2}}$ from (17).
- Calculate $u_{l+\frac{1}{2}}^{n+1}$ for $l = 0, \ldots, N-1$, from (8a).

At this point the updating cycle is complete, and the procedure repeats, after shifting data. Proponents of wave digital filtering often call attention to this computability issue, usually dealt with using

so-called reflection-free ports [3]. One may see here that the same property is available using finite difference schemes, and furthermore, numerical solution uniqueness may be ensured (in contrast with wave digital methods making use of nonlinear elements, and power-normalized waves [26]).

3.4. Numerical Stability

The question of numerical stability of the simulation as a whole is a delicate one, but may be dealt with using energy concepts [25], which have already been applied to variety of other nonlinear musical systems, such as string [27] and plate vibration [28]; it is, however, too large a topic to cover sufficiently in a short publication. In fact, one may definitively prove numerical stability (i.e., boundedness of computed solutions under any possible set of reed and tube parameters, and for any pressure excitation waveform) in the absence of the collision term in (3)—stability under collision conditions is notoriously difficult to show, but the use of a semi-implicit discretization is an excellent ad hoc means of preventing such difficulties. The key point, however, is that if a scheme such as (8) is employed over the domain interior, and the Courant condition (11) is obeyed, then a connection with semi-implicit approximations to energetically well-behaved objects such as the reed or bell termination, there is no further condition necessary. A fuller sketch of numerical stability results for this system will appear in a forthcoming publication [25].

3.5. Computational Considerations

The computational cost of this algorithm is almost entirely due to the updating of the scheme for the tube, and, as such, is governed by the choice of time step k and grid spacing h, which are related by the CFL condition (11). The condition should be fulfilled as close to equality as possible—otherwise, excessive numerical dispersion, leading to mode mistuning and a severe limitation in audio bandwidth [25] will result. Thus, for a given time step $k = 1/f_s$, the memory requirement will be almost exactly $2f_s/\gamma = 2f_sL/c$ units. Updating at a single grid point requires three arithmetic operations, and thus the total operation count will be $6f_s^2/\gamma = 6Lf_s^2/c$ operations/second. For typical wind instruments, and at a suitably high audio sample rate, such as $f_s = 44100$ Hz, the operation count will be on the order of tens of megaoperations/second, well within real time capability on a modest laptop computer. (For example, on the author's laptop, a Dell with a 2.0 GHz Pentium, and for the case of a clarinet geometry, it takes approximately 3.9 s to generate 5 s of sound output, at 44.1 kHz, in Matlab.) On the other hand, it is more expensive, in terms of arithmetic (though not memory) than a typical waveguide algorithm.

4. SIMULATION RESULTS

4.1. Bore Profiles

It is particularly simple, in the direct FD framework, to alter the bore profile—the function $S(x)$ may be set arbitrarily, and once set, values of the function are used, without further calculations (as of scattering coefficients or impedances) in the simulation. It is thus straightforward to experiment with bore profiles which may differ substantially from, e.g., those which lead to efficient waveguide realizations. See Figure 4. In particular, computational effort is independent of the choice of bore profile.

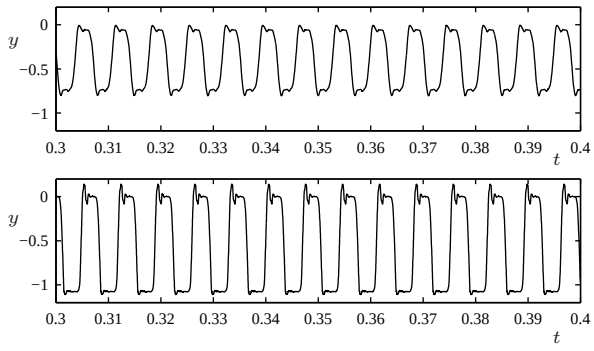

Figure 5: *Non-dimensional reed displacement y, for a clarinetlike configuration, of parameters as given in the caption to Figure 4, and with a bore profile as shown in Figure 4(b). The parameters for the collision term in* (3) *are chosen as $\omega_1 = 316$, and the nonlinearity exponent is $\alpha = 4$. In (a), the input is a steady nondimensional mouth pressure of $p_m = 0.013$, and in (b), $p_m = 0.02$.*

4.2. Reed Beating

As an example of typical phenomena generated by such a model, consider the perceptually important reed-beating effect, as illustrated in Figure 5. In particular, note that the nondimensional reed displacement takes on values < -1; the extent of such "penetration" may be controlled through the choice of ω_1 and α, but the general results are in agreement with other published results (see, e.g., [29]).

4.3. Onset Times

As another example, the variation in onset times for notes as a function of mouth pressure, characteristic of wind instruments, is shown in Figure 6.

Sound examples will be available shortly at the authors web address [30].

5. GRAPHICAL USER INTERFACE

A graphical user interface has been developed for this synthesis algorithm, using the development tool (GUIDE) in the Matlab programming environment. The user is able to set all reed parameters, the form of the pressure ecitation, and a variety of reasonable choices are available for the tube itself, including the usual cylinder and cone profiles, as well as additional bell geometry specifications. It is also possible to toggle between reed and brass models, and, in the case of brass instruments, to specify a time-varying lip stiffness. See Figure 7. The user interface will be made publicly available in the near future.

6. CONCLUSION

Perhaps the greatest advantage of a fully discrete formulation is fidelity to the physics of the continuous time/space model itself; as a result, many issues which appear in more efficient designs, such as "lumping" of impedances, fractional delay interpolation, etc., may be sidestepped. Another advantage is extensibility—see below for some examples. The greatest disadvantage is computational cost,

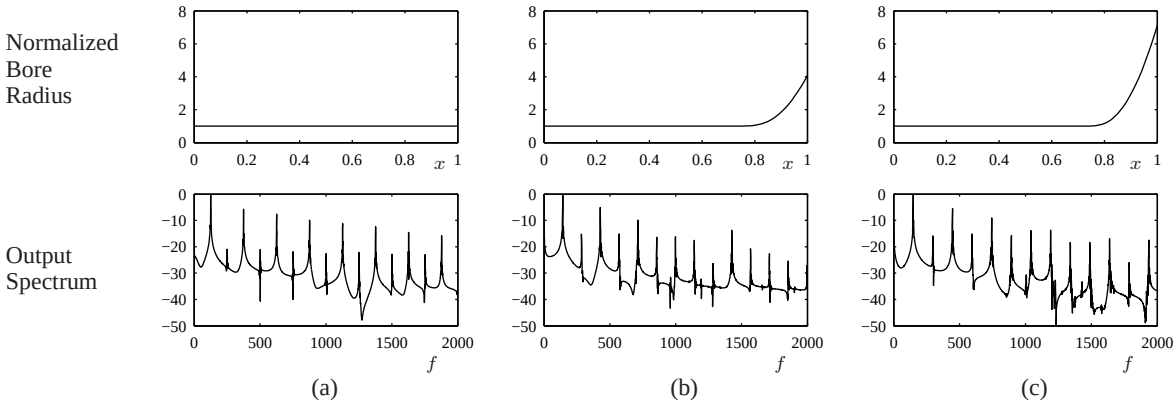

Figure 4: *Typical output spectra, for various bore types: (a) a cylinder, (b) a cylinder with a clarinet-like bell, and (c) a cylinder with a bell of extreme flare. In each case, the other model parameters correspond, roughly, to those of a clarinet:* $\gamma = 512$, $\mathcal{Q} = 1.6 \times 10^{10}$, $\mathcal{R} = 0.032$, $\mathcal{S} = 10^{-6}$, $\omega_0 = 23250$, $g = 3000$.

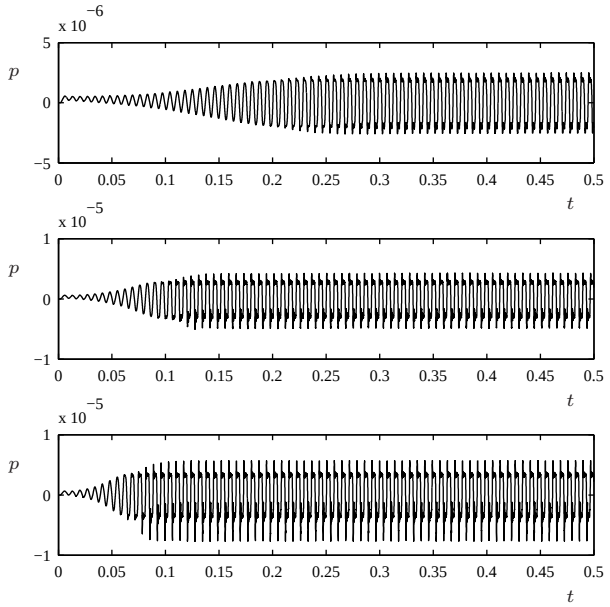

Figure 6: *Non-dimensional output pressure, for the wind model of parameters given in the caption to Figure 4, and using the clarinet-like bore profile shown in Figure 4(b). Top, with a nondimensional mouth pressure of* $p_m = 0.01$, *center, with* $p_m = 0.015$, *and bottom, with* $p_m = 0.02$.

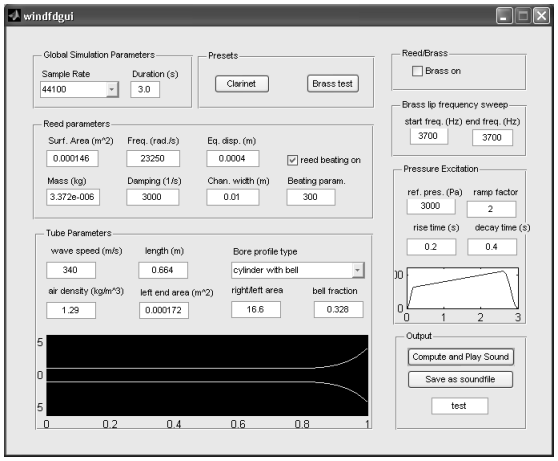

Figure 7: *Graphical user interface for the wind synthesis algorithm.*

which is, in fact, not extremely high, though certainly higher than that of, e.g., a waveguide model.

There are many ways in which the FD wind model here should be extended. Several are in progress, and have not been discussed in this short paper—in particular, there is a simple extension to "blown open" brass-like instruments which is nearly trivial, involving only a single change in polarity of the pressure difference Δp in the model. Such a feature is already included in the GUI mentioned in Section 5. In addition, it is rather straightforward to implement models of woodwind toneholes [31, 32], without the usual concern of commuting or lumping of impedances in instruments of more complex bore profile. Another obvious step is the porting of such an algorithm to a real time environment such as Max/MSP [33] or csound [34]—as noted earlier, a real time implementation is easily possible, and such developments are under way.

Other extensions are also possible. The fully discrete FD approach is very well suited to an extension to nonlinear 1D wave propagation—the linearity hypothesis is probably sufficient for reed

instruments, and brass instruments under moderate amplitude excitation, though nonlinear effects do appear at high amplitudes in instruments such as the trombone [35]. Fully discrete methods in computing shock wave solutions have a very long history in mainstream fluid dynamics applications—see, e.g., the text by Hirsch [36], or the classic article by Sod [37]. The introduction of loss in the acoustic tube, however, is in some ways more problematic. Often, loss in the boundary layer of a tube is modelled in the frequency domain, leading to a square root frequency dependence—when transformed back to the time domain, one arrives at a PDE involving fractional derivatives, which cause immense difficulty numerically, though discrete models of loss have been examined in great detail, in the scattering context, by Matignon [38]. Finally, the model described here is generally valid when bore radius is small compared to audio wavelengths, and when its spatial variation is not too great. In such cases, one may need to resort to models of wave propagation incorporating higher modes, and possibly mode conversion. In the fully discrete case, one could employ a three-dimensional model of the tube, with a very coarse grid approximation in the transverse direction, and another approach might involve multimodal propagation models.

7. REFERENCES

[1] J. O. Smith III, "Efficient simulation of the reed-bore and bow-string mechanisms," in *Proceedings of the International Computer Music Conference*, The Hague, The Netherlands, 1986, pp. 275–280.

[2] G. Scavone, *An Acoustic Analysis of Single-Reed Woodwind Instruments with an Emphasis on Design and Performance Issues and Digital Waveguide Techniques*, Ph.D. thesis, Department of Music, Stanford University, 1997.

[3] A. Fettweis, "Wave digital filters: Theory and practice," *Proceedings of the IEEE*, vol. 74, no. 2, pp. 270–327, February 1986.

[4] S. Bilbao, J. Bensa, and R. Kronland-Martinet, "The wave digital reed: A passive formulation," in *Proceedings of the COST-G6 Digital Audio Effects Conference*, London, England, September 2003, pp. 225–230.

[5] M. van Walstijn and G. Scavone, "The wave digital tonehole model," in *Proceedings of the International Computer Music Conference*, Berlin, Germany, August 2000, pp. 465–468.

[6] P. Guillemain, "A digital synthesis model of double-reed wind instruments," *EURASIP Journal of Applied Signal Processing*, vol. 7, pp. 990–1000, 2004.

[7] F. Avanzini and D. Rocchesso, "Efficiency, accuracy, and stability issues in discrete time simulations of single reed instruments," *Journal of the Acoustical Society of America*, vol. 111, no. 5, pp. 2293–2301, 2002.

[8] M. McIntyre, R. Schumacher, and J. Woodhouse, "On the oscillations of musical instruments," *Journal of the Acoustical Society of America*, vol. 74, no. 5, pp. 1325–1345, 1983.

[9] D. Noreland, *Numerical Techniques for Acoustic Modelling and Design of Brass Wind Instruments*, Ph.D. thesis, Uppsala University, 2003.

[10] P. Morse and U. Ingard, *Theoretical Acoustics*, Princeton University Press, Princeton, New Jersey, 1968.

[11] N. Fletcher and T. Rossing, *The Physics of Musical Instruments*, Springer-Verlag, New York, New York, USA, 1991.

[12] L. Rabiner and R. Schafer, *Digital Processing of Speech Signals*, Prentice-Hall, Englewood Cliffs, New Jersey, USA, 1978.

[13] J. L. Kelly and C. C. Lochbaum, "Speech synthesis," in *Proceedings of the Fourth International Congress on Acoustics*, Copenhagen, Denmark, 1962, pp. 1–4, Paper G42.

[14] A. Chaigne and A. Askenfelt, "Numerical simulations of struck strings. I. A physical model for a struck string using finite difference methods," *Journal of the Acoustical Society of America*, vol. 95, no. 2, pp. 1112–1118, February 1994.

[15] J. Kergomard P. Guillemain and T. Voinier, "Real-time synthesis of clarinet-like instruments using digital impedance models," *Journal of the Acoustical Society of America*, vol. 118, no. 1, pp. 483–494, 2005.

[16] J. Kergomard, *Elementary Considerations on Reed-instrument Oscillations*, Springer, New York, New York, USA, 1995.

[17] T. Tachibana and K. Takahashi, "Sounding mechanism of a cylindrical pipe fitted with a clarinet mouthpiece," *Progress of Theoretical Physics*, vol. 104, no. 2, pp. 265–288, 2000.

[18] J. Backus, "Small vibration theory of the clarinet," *Journal of the Acoustical Society of America*, vol. 35, pp. 305–313, 1963.

[19] M. Atig, J.-P. Dalmont, and J. Gilbert, "Termination impedance of open-ended cylindrical tubes at high sound pressure level," *Comptes Rendus Mecanique*, vol. 332, pp. 299.

[20] V. Belevitch, *Classical Network Theory*, Holden Day, San Francisco, California, USA, 1968.

[21] K. S. Yee, "Numerical solution of initial boundary value problems involving Maxwell's equations in isotropic media," *IEEE Transactions on Antennas and Propagation*, vol. 14, pp. 302–307, 1966.

[22] A. Taflove, *Computational Electrodynamics*, Artech House, Boston, Massachusetts, USA, 1995.

[23] J. Strikwerda, *Finite Difference Schemes and Partial Differential Equations*, Wadsworth and Brooks/Cole Advanced Books and Software, Pacific Grove, California, USA, 1989.

[24] R. Courant, K. Friedrichs, and H. Lewy, "Über die partiellen differenzengleichungen de mathematischen Physik," *Mathematische Annalen*, vol. 100, pp. 32–74, 1928.

[25] S. Bilbao, *Numerical Sound Synthesis*, John Wiley and Sons, Chichester, UK, 2008, Under contract, due for publication in September, 2008.

[26] S. Bilbao, *Wave and Scattering Methods for Numerical Simulation*, John Wiley and Sons, Chichester, UK, 2004.

[27] S. Bilbao and J. O. Smith III, "Energy conserving finite difference schemes for nonlinear strings," *Acustica*, vol. 91, pp. 299–311, 2005.

[28] S. Bilbao, "A family of conservative finite difference schemes for the dynamical von Karman plate equations," *Numerical Methods for Partial Differential Equations*, vol. 24, no. 1, pp. 193–216, 2008.

[29] D. Keefe, "Physical modeling of wind instruments," *Computer Music Journal*, vol. 16, no. 4, pp. 57–73, 1992.

[30] S. Bilbao, ," Sound synthesis examples available online at http://www.music.ed.ac.uk/Contacts/DrStefanBilbao_soundExamples.htm.

[31] V. Välimäki, M. Karjalainen, and T. Laakso, "Modeling of woodwind bores with finger holes," in *Proceedings of the International Computer Music Conference*, Tokyo, 1993, pp. 32–39.

[32] D. Keefe, "Theory of the single woodwind tone hole. experiments on the single woodwind tone hole," *Journal of the Acoustical Society of America*, vol. 72, pp. 676–699, 1982.

[33] D. Zicarelli, "How I learned to love a program that does nothing," *Computer Music Journal*, vol. 26, no. 4, pp. 44–51, 2002.

[34] R. Boulanger, Ed., *The csound Book: Perspectives in Software Synthesis, Sound Design, Signal Processing,and Programming*, MIT Press, Cambridge, Massachusetts, 2001.

[35] A. Hirschberg, J. Gilbert, R. Msallam, and A. Wijnands, "Shock waves in trombones," *Journal of the Acoustical Society of America*, vol. 99, no. 3, pp. 1754–1758, 1996.

[36] C. Hirsch, *Numerical Computation of Internal and External Flows*, John Wiley and Sons, Chichester, England, 1988.

[37] G. Sod, "A survey of several finite difference methods for systems of nonlinear hyperbolic conservation laws," *Journal of Computational Physics*, vol. 27, no. 1, pp. 1–31, April 1978.

[38] D. Matignon, *State-space representations of waveguide models with fractional derivatives*, Ph.D. thesis, Paris, France, 1994.